

Quasiclassical fluctuations of the superconductor proximity gap in a chaotic system

M.C. Goorden, Ph. Jacquod*, and C.W.J. Beenakker

Instituut-Lorentz, Universiteit Leiden, P.O. Box 9506, 2300 RA Leiden, The Netherlands

(Dated: 30 June 2003)

We calculate the sample-to-sample fluctuations in the excitation gap of a chaotic dynamical system coupled by a narrow lead to a superconductor. Quantum fluctuations on the order of magnitude of the level spacing, predicted by random-matrix theory, apply if $\tau_E \ll \hbar/E_T$ (with τ_E the Ehrenfest time and E_T the Thouless energy). For $\tau_E \gtrsim \hbar/E_T$ the fluctuations are much greater than the level spacing. We demonstrate the quasiclassical nature of the gap fluctuations in the large- τ_E regime by correlating them to an integral over the classical dwell-time distribution.

PACS numbers: 74.45.+c, 03.65.Sq, 05.45.Mt, 74.78.Na

The universality of statistical fluctuations is one of the most profound manifestations of quantum mechanics in mesoscopic systems [1]. Classically, the conductance g of a disordered metal (measured in the fundamental unit $2e^2/h$) would fluctuate from sample to sample by an amount of order $(l/L)^{3/2} \ll 1$, with l the mean free path and L the length of the conductor [2]. Quantum mechanical interference increases the fluctuations to order unity, independent of disorder or sample length. This is the phenomenon of universal conductance fluctuations [3, 4]. The same universality applies to a variety of other properties of disordered metals and superconductors, and random-matrix theory (RMT) provides a unified description [5].

Chaotic systems (for example, a quantum dot in the shape of a stadium) share much of the phenomenology of disordered systems: The same universality of sample-to-sample fluctuations exists [6, 7, 8]. What is different is the appearance of a new time scale, below which RMT breaks down [9, 10]. This time scale is the Ehrenfest time τ_E , which measures how long it takes for a wave packet of minimal size to expand over the entire available phase space. If τ_E is larger than the mean dwell time τ_D in the system (the reciprocal of the Thouless energy $E_T = \hbar/2\tau_D$), then interference effects are inoperative. A chaotic system with conductance $g \times 2e^2/h$, level spacing δ , and Lyapunov exponent λ has $\tau_D = 2\pi\hbar/g\delta$ and $\tau_E = \lambda^{-1} \ln(g\tau_0/\tau_D)$, with τ_0 the time of flight across the system [11]. The defining characteristic of the Ehrenfest time is that it scales logarithmically with \hbar , or equivalently, logarithmically with the system size over Fermi wavelength [12].

The purpose of this paper is to investigate what happens to mesoscopic fluctuations if the Ehrenfest time becomes comparable to, or larger than, the dwell time, so one enters a quasiclassical regime where RMT no longer holds. This quasiclassical regime has not yet been explored experimentally. The difficulty is that τ_E increases so slowly with system size that the averaging effects of

inelastic scattering take over before the effect of a finite Ehrenfest time can be seen. In a computer simulation inelastic scattering can be excluded from the model by construction, so this seems a promising alternative to investigate the crossover from universal quantum fluctuations to nonuniversal quasiclassical fluctuations. Contrary to what one would expect from the disordered metal [2], where quasiclassical fluctuations are much smaller than the quantum value, we find that the breakdown of universality in the chaotic system is associated with an *enhancement* of the sample-to-sample fluctuations.

The quantity on which we choose to focus is the excitation gap ε_0 of a chaotic system which is weakly coupled to a superconductor. We have two reasons for this choice: Firstly, there exists a model (the Andreev kicked rotator) which permits a computer simulation for systems large enough that $\tau_E \gtrsim \tau_D$. So far, such simulations, have confirmed the microscopic theory of Ref. [11] for the average gap $\langle \varepsilon_0 \rangle$ [13]. Secondly, there exists a quasiclassical theory for the effect of a finite Ehrenfest time on the excitation gap and its fluctuations [14]. This allows us to achieve both a numerical and an analytical understanding of the mesoscopic fluctuations when RMT breaks down.

We summarize what is known from RMT for the gap fluctuations [15]. In RMT the gap distribution $P(\varepsilon_0)$ is a universal function of the rescaled energy $(\varepsilon_0 - E_g)/\Delta_g$, where $E_g = 0.6 E_T$ is the mean-field energy gap and $\Delta_g = 0.068 g^{1/3} \delta$ determines the mean level spacing just above the gap. The distribution function has mean $\langle \varepsilon_0 \rangle = E_g + 1.21 \Delta_g$ and standard deviation $(\langle \varepsilon_0^2 \rangle - \langle \varepsilon_0 \rangle^2)^{1/2} \equiv \delta\varepsilon_{\text{RMT}}$ given by

$$\delta\varepsilon_{\text{RMT}} = 1.27\Delta_g = 1.09 E_T/g^{2/3}. \quad (1)$$

The RMT predictions for $P(\varepsilon_0)$, in the regime $\tau_E \ll \tau_D$, were confirmed numerically in Ref. [13] using the Andreev kicked rotator.

We will use the same model, this time focusing on the gap fluctuations $\delta\varepsilon_0$ in the regime $\tau_E \gtrsim \tau_D$. The Andreev kicked rotator provides a stroboscopic description (period τ_0) of the dynamics in a normal region of phase space (area $M\hbar_{\text{eff}}$) coupled to a superconductor in a much smaller region (area $N\hbar_{\text{eff}}$, $1 \ll N \ll M$). We re-

*Present address: Department of Theoretical Physics, University of Geneva, 24 Quai Ernest Ansermet, CH-1211 Geneva 4, Switzerland.

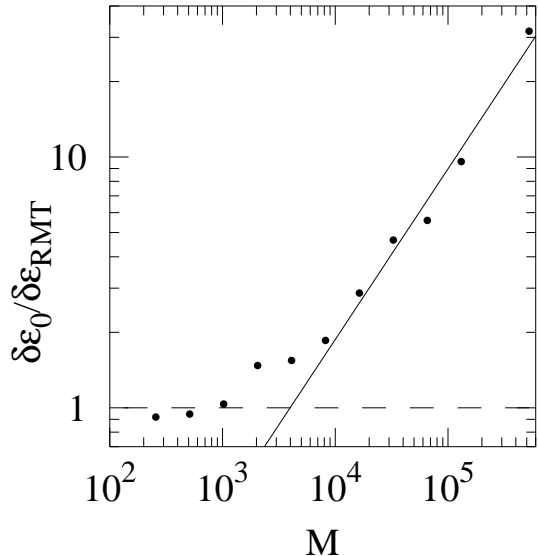


FIG. 1: Root-mean-square value $\delta\varepsilon_0$ of the gap divided by the RMT prediction $\delta\varepsilon_{\text{RMT}}$, as a function of the system size M for dwell time $M/N = 5$ and kicking strength $K = 14$. The data points result from the numerical simulation of the Andreev kicked rotator. The solid line has slope $2/3$, indicating that $\delta\varepsilon_0$ depends only on M/N and not on M or N separately in the large- M regime.

fer to this coupling as a “lead”. The effective Planck constant is $\hbar_{\text{eff}} = 1/M$. The mean dwell time in the normal region (before entering the lead) is $\tau_D = M/N$ and the corresponding Thouless energy is $E_T = N/2M$. We have set τ_0 and \hbar equal to 1. The dimensionless conductance of the lead is $g = N$. The product $\delta = 4\pi E_T/g = 2\pi/M$ is the mean spacing of the quasi-energies ε_m of the normal region without the coupling to the superconductor. The phase factors $e^{i\varepsilon_m}$ ($m = 1, 2, \dots, M$) are the eigenvalues of the Floquet operator F , which is the unitary matrix that describes the dynamics in the normal region. In the model of the kicked rotator the matrix elements of F in momentum representation are given by [16]

$$F_{nm} = e^{-(i\pi/2M)(n^2+m^2)}(UQU^\dagger)_{nm}, \quad (2a)$$

$$U_{nm} = M^{-1/2}e^{(2\pi i/M)nm}, \quad (2b)$$

$$Q_{nm} = \delta_{nm}e^{-(iMK/2\pi)\cos(2\pi n/M)}. \quad (2c)$$

The coupling to the superconductor doubles the dimension of the Floquet operator, to accommodate both electron and hole dynamics. The scattering from electron to hole, known as Andreev reflection, is described by the matrix

$$\mathcal{P}^{1/2} = \begin{pmatrix} 1 - (1 - \frac{1}{2}\sqrt{2})P^T P & -i\frac{1}{2}\sqrt{2}P^T P \\ -i\frac{1}{2}\sqrt{2}P^T P & 1 - (1 - \frac{1}{2}\sqrt{2})P^T P \end{pmatrix}, \quad (3)$$

with the projection operator

$$(P^T P)_{nm} = \delta_{nm} \times \begin{cases} 1 & \text{if } L \leq n \leq L + N - 1, \\ 0 & \text{otherwise.} \end{cases} \quad (4)$$

Since we work in momentum representation, the lead defined by Eq. (4) is a strip in phase space of width N parallel to the coordinate axis. One could alternatively consider a lead parallel to the momentum axis, if one would work in coordinate representation. We do not expect any significant differences between the two alternatives. Putting all this together we arrive at the Floquet operator of the Andreev kicked rotator [13],

$$\mathcal{F} = \mathcal{P}^{1/2} \begin{pmatrix} F & 0 \\ 0 & F^* \end{pmatrix} \mathcal{P}^{1/2}. \quad (5)$$

The matrix \mathcal{F} can be diagonalized efficiently using the Lanczos technique in combination with the Fast-Fourier-Transform algorithm [17]. This makes it possible to calculate the quasi-energies ε_m and eigenfunctions ψ_m for systems of sizes up to $M = 5 \cdot 10^5$. The gap value ε_0 is given by the eigenphase of \mathcal{F} closest to zero.

The Floquet operator (5) provides a stroboscopic description of the electron and hole dynamics, which is believed to be equivalent to the true Hamiltonian dynamics on long time scales $t \gg \tau_0$. The support for this comes from two sides: (i) In the absence of superconductivity, and for varying parameters K and \hbar_{eff} , the 1-D kicked rotator correctly reproduces properties of localized [18], diffusive [19], and even ballistic [20] quasiparticles in disordered media. (ii) In the presence of superconductivity, the kicked Andreev rotator, and extensions thereof, adequately describe quantum dots in contact with a superconductor [13], and give a proper description of quasiparticles in dirty d-wave superconductors [21]. Since we will be giving a classical interpretation of our results, we also describe the classical map corresponding to the Andreev kicked rotator. The map relates the dimensionless coordinate $x_n \in (0, 1)$ and momentum $p_n \in (0, 1)$ at time $(n+1)\tau_0$ to the values at time $n\tau_0$:

$$p_{n+1} = p_n \pm (K/2\pi) \sin[2\pi(x_n \pm \frac{p_n}{2})], \quad (6a)$$

$$x_{n+1} = x_n \pm \frac{p_n}{2} \pm \frac{p_{n+1}}{2}. \quad (6b)$$

The upper and lower sign correspond to electron and hole dynamics, respectively. Periodic boundary conditions hold both for x and p . The quasiparticle reaches the superconductor if $|p_{n+1} - p_{\text{lead}}| < N/2M$, where p_{lead} is the center of the lead. At the next iteration the electron is converted into a hole and vice versa.

We study a system with kicking strength $K = 14$ (fully chaotic, Lyapunov exponent $\lambda = 1.95$) and vary the level spacing $\delta = 2\pi/M$ at fixed dwell time $\tau_D = M/N = 5$. Sample-to-sample fluctuations are generated by varying the position p_{lead} of the lead over some 400 locations. The resulting M -dependence of $\delta\varepsilon_0$ is plotted in Fig. 1 on a double logarithmic scale. We have divided the value $\delta\varepsilon_0$ resulting from the simulation by the RMT prediction $\delta\varepsilon_{\text{RMT}}$ from Eq. (1). The numerical data follows this prediction for $M \lesssim 10^3$, but for larger M the fluctuations are bigger than predicted by RMT. For $M \gtrsim 10^4$ the ratio $\delta\varepsilon_0/\delta\varepsilon_{\text{RMT}}$ grows as $M^{2/3}$ (solid line). Since $\delta\varepsilon_{\text{RMT}} \propto$

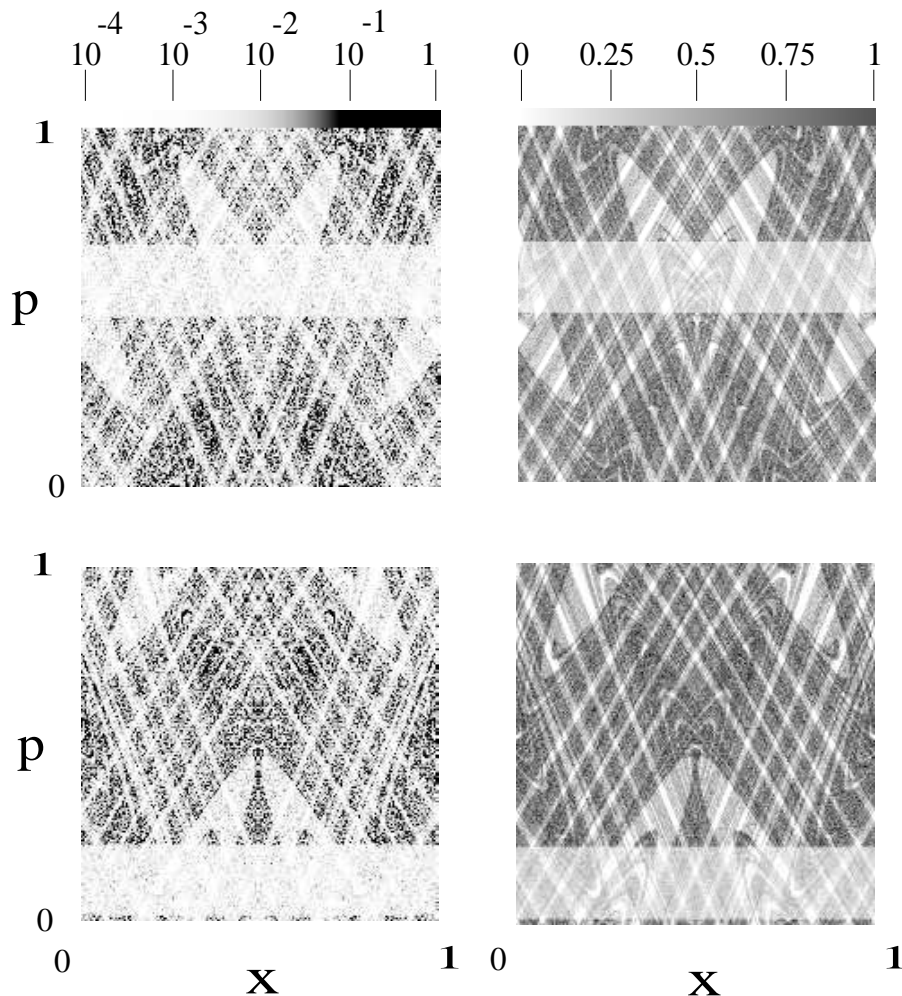


FIG. 2: Left panels: Husimi function (7) for the electron component of the ground-state wavefunction ψ_0 of the Andreev kicked rotator, for two different positions of the lead. The parameters are $M = 131072$, $\tau_D = M/N = 5$, $K = 14$. The calculated values are scaled by a factor 0.019 (0.017) in the top (bottom) panel, so that they cover the range (0,1), indicated by the gray scale at the top. Right panels: The corresponding classical density plots of all trajectories which have a time $t > 7$ between Andreev reflections. The calculated values are rescaled by a factor 0.30 (0.32) in the top (bottom) panel.

$M^{-2/3}$, this means that $\delta\varepsilon_0$ is independent of the level spacing $\delta = 2\pi/M$ at fixed dwell time $\tau_D = M/N$. This suggests a quasiclassical explanation.

To relate the fluctuations of ε_0 to the classical dynamics, we first examine the corresponding wavefunction ψ_0 . In the RMT regime the wavefunctions are random and show no features of the classical trajectories. In the quasiclassical regime $\tau_E \gtrsim \tau_D$ we expect to see some classical features. Phase space portraits of the electron components ψ_m^e of the wavefunctions are given by the Husimi function

$$\mathcal{H}(n_x, n_p) = |\langle \psi_m^e | n_x, n_p \rangle|^2. \quad (7)$$

The state $|n_x, n_p\rangle$ is a Gaussian wave packet centered at $x = n_x/M$, $p = n_p/M$. In momentum representation it reads

$$\langle n | n_x, n_p \rangle \propto e^{-\pi(n-n_p)^2/M} e^{2\pi i n_x n/M}. \quad (8)$$

In Fig. 2, left panels, the Husimi function of ψ_0 is shown for two lead positions. Shown is a logarithmic gray scale density plot of the Husimi function, with light (dark) areas corresponding to low (high) density. The lead is visible as a light strip parallel to the x -axis. It is clear that these wavefunctions are not random. We expect that the structure that one sees corresponds to long classical trajectories, since the wavefunctions are for the lowest quasi-energy. To test this expectation, we show in the right panels (on a linear gray scale) the corresponding classical density plots for all trajectories with dwell time $t > t^*$. A total of $3 \cdot 10^5$ initial conditions (x_0, p_0) for these trajectories are chosen uniformly in the lead. Each new iteration of the map (6) gives a point (x_n, p_n) in phase space, which is kept if the time of return to the lead is greater than t^* . We take $t^* = 7$, somewhat larger than the Ehrenfest time $\tau_E = \lambda^{-1} \ln(N^2/M) = 4.4$. The

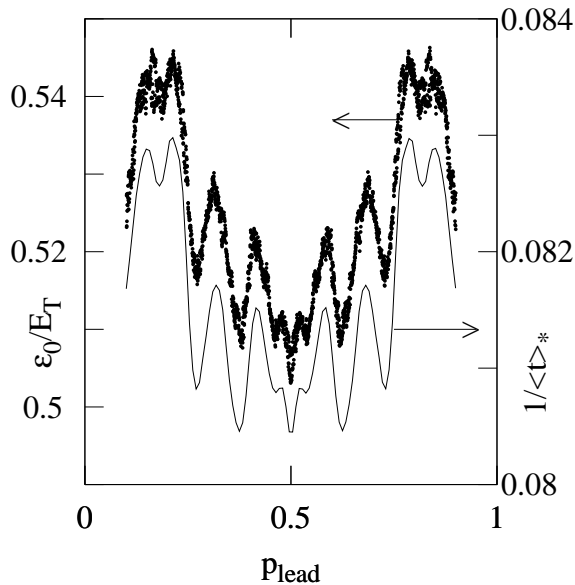


FIG. 3: The data points (left axis) are the quantum mechanical gap values ε_0 of the Andreev kicked rotorator as a function of the position p_{lead} of the lead, for parameter values $M = 131072$, $\tau_D = M/N = 5$, $K = 14$. The solid line (right axis) is the reciprocal of the mean dwell time $\langle t \rangle_* = \int_{t^*}^{\infty} tP(t)dt / \int_{t^*}^{\infty} P(t)dt$ of classical trajectories longer than $t^* = 7$.

plot is not particularly sensitive to the value of t^* , as long as $t^* > \tau_E$. There is a clear correspondence between the quantum mechanical Husimi function and the classical density plot. We conclude that the wavefunction of the lowest excitation covers predominantly that part of phase space where the longest dwell times occur.

To make this more quantitative we show in Fig. 3 the gap value from the quantum simulations as a function of the lead position. The solid curve results from a classical calculation of the mean dwell time of those trajectories with $t > t^*$, for the same value $t^* = 7$ used in Fig. 2.

More precisely, it is a plot of

$$\frac{1}{\langle t \rangle_*} = \frac{\int_{t^*}^{\infty} P(t)dt}{\int_{t^*}^{\infty} tP(t)dt}, \quad (9)$$

with $P(t)$ the classical dwell time distribution. We see that the sample-to-sample fluctuations in the gap ε_0 correlate very well with the fluctuations in the sample-to-sample mean dwell time of long trajectories. Again, the correlation is not sensitive to the choice $t^* > \tau_E$. Such a correlation is in accord with recent theoretical work [14], in which an effective RMT description is expected to hold for the part of phase space with dwell times greater than the Ehrenfest time. But we should emphasize that the agreement is only qualitative. In particular, the relation $\varepsilon_0 \approx 1.5/\langle t \rangle_* - 0.07$ that we infer from Fig. 3 is different from the relation $\varepsilon_0 = 0.3/\langle t \rangle_*$ that would be expected from RMT. While the theory of Ref. [11] has been found to be in good agreement with the average gap value $\langle \varepsilon_0 \rangle$ [13], it is not clear how it compares to the data of Fig. 3.

In conclusion, we have investigated the transition from quantum mechanical to quasiclassical gap fluctuations in the superconductor proximity effect. The transition is accompanied by a loss of universality and a substantial enhancement of the fluctuations. Our numerical data provides qualitative support for an effective random-matrix theory in a reduced part of phase space [14], as is witnessed by the precise correlation which we have found between the value of the gap and the dwell time of long classical trajectories (see Fig. 3). It would be of interest to investigate to what extent quasiclassical fluctuations of the conductance in a ballistic chaotic system are similar or different from those of the superconducting gap studied here.

We have benefitted from discussions with J. Tworzydło. This work was supported by the Dutch Science Foundation NWO/FOM and the Swiss National Science Foundation.

-
- [1] Y. Imry, *Introduction to Mesoscopic Physics* (Oxford University, Oxford, 1997).
 - [2] Yu.M. Galperin and V.I. Kozub, *Europhys. Lett.* **15**, 631 (1991).
 - [3] B.L. Altshuler, *JETP Lett.* **41**, 648 (1985).
 - [4] P.A. Lee and A.D. Stone, *Phys. Rev. Lett.* **55**, 1622 (1985).
 - [5] C.W.J. Beenakker, *Phys. Rev. B* **47**, 15763 (1993).
 - [6] C.W.J. Beenakker, *Rev. Mod. Phys.* **69**, 731 (1997).
 - [7] T. Guhr, A. Müller-Groeling, and H.A. Weidenmüller, *Phys. Rep.* **299**, 189 (1998).
 - [8] Y. Alhassid, *Rev. Mod. Phys.* **72**, 895 (2000).
 - [9] A. Lodder and Yu. V. Nazarov, *Phys. Rev. B* **58**, 5783 (1998).
 - [10] I.L. Aleiner and A.I. Larkin, *Phys. Rev. B* **54**, 14423 (1996).
 - [11] M.G. Vavilov and A.I. Larkin, *Phys. Rev. B* **67** 115335 (2003).
 - [12] G.M. Zaslavsky, *Phys. Rep.* **80**, 157 (1981).
 - [13] Ph. Jacquod, H. Schomerus, and C.W.J. Beenakker, *Phys. Rev. Lett.* **90**, 207004 (2003).
 - [14] P.G. Silvestrov, M.C. Goorden, and C.W.J. Beenakker, *Phys. Rev. Lett.* **90**, 116801 (2003).
 - [15] M.G. Vavilov, P.W. Brouwer, V. Ambegaokar, and C.W.J. Beenakker, *Phys. Rev. Lett.* **86**, 874 (2001).
 - [16] F.M. Izrailev, *Phys. Rep.* **196**, 299 (1990).
 - [17] R. Ketzmerick, K. Kruse, and T. Geisel, *Physica D* **131**, 247 (1999).
 - [18] S. Fishman, D. R. Grempel, and R. E. Prange, *Phys. Rev. Lett.* **49**, 509 (1984).
 - [19] A. Altland and M. R. Zirnbauer, *Phys. Rev. Lett.* **77**, 4536 (1996).

- [20] J. Tworzydło, A. Tajic, H. Schomerus, and C.W.J. Beenakker, cond-mat/0304327.
- [21] Í. Adagideli and Ph. Jacquod, cond-mat/0307159.